

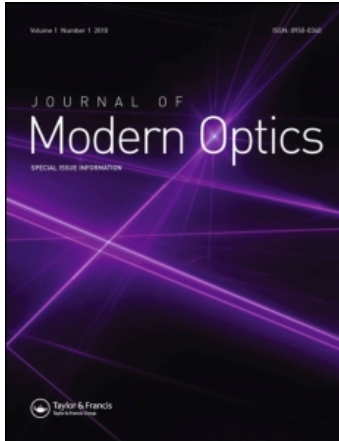
This article was downloaded by: [Weizman Institute]

On: 26 July 2010

Access details: Access Details: [subscription number 919693000]

Publisher Taylor & Francis

Informa Ltd Registered in England and Wales Registered Number: 1072954 Registered office: Mortimer House, 37-41 Mortimer Street, London W1T 3JH, UK



Journal of Modern Optics

Publication details, including instructions for authors and subscription information:

<http://www.informaworld.com/smpp/title~content=t713191304>

Two-dimensional phase-only spatial light modulators for dynamic phase and amplitude pulse shaping

E. Frumker^{ab}; Y. Silberberg^c

^a SIMS NRC, Ottawa, Canada ^b Physics Department, Texas A&M University, College Station, USA ^c Department of Physics of Complex Systems, Weizmann Institute of Science, Rehovot, Israel

First published on: 12 August 2009

To cite this Article Frumker, E. and Silberberg, Y.(2009) 'Two-dimensional phase-only spatial light modulators for dynamic phase and amplitude pulse shaping', Journal of Modern Optics, 56: 18, 2049 – 2054, First published on: 12 August 2009 (iFirst)

To link to this Article: DOI: 10.1080/09500340903199913

URL: <http://dx.doi.org/10.1080/09500340903199913>

PLEASE SCROLL DOWN FOR ARTICLE

Full terms and conditions of use: <http://www.informaworld.com/terms-and-conditions-of-access.pdf>

This article may be used for research, teaching and private study purposes. Any substantial or systematic reproduction, re-distribution, re-selling, loan or sub-licensing, systematic supply or distribution in any form to anyone is expressly forbidden.

The publisher does not give any warranty express or implied or make any representation that the contents will be complete or accurate or up to date. The accuracy of any instructions, formulae and drug doses should be independently verified with primary sources. The publisher shall not be liable for any loss, actions, claims, proceedings, demand or costs or damages whatsoever or howsoever caused arising directly or indirectly in connection with or arising out of the use of this material.

Two-dimensional phase-only spatial light modulators for dynamic phase and amplitude pulse shaping

E. Frumker^{a,b,*} and Y. Silberberg^c

^a*SIMS NRC, Ottawa, Canada;* ^b*Physics Department, Texas A&M University, College Station, USA;*

^c*Department of Physics of Complex Systems, Weizmann Institute of Science, Rehovot, Israel*

(Received 21 February 2009; final version received 22 July 2009)

We consider a two-dimensional liquid crystal spatial light modulator (SLM) for femtosecond pulse shaping. Novel shaping schemes enabling a drastic speed increase (about four orders of magnitude as compared with conventional liquid-crystal SLM-based pulse shapers) and complex (phase and amplitude) femtosecond pulse shaping are discussed and experimentally demonstrated. In the first case, while a horizontal resolution of 1920 addressable pixels provided superior fidelity for generating complex waveforms, scanning across the vertical dimension (1080 pixels) has been used to facilitate an update rate in excess of 100 kHz. In the second case, we use the pixel count redundancy in the vertical direction and encode a spectrally-dependent diffraction grating for modulation of both spectral phases and amplitudes.

Keywords: femtosecond pulse shaping; spatial light modulators; ultrafast science; coherent control; non-linear microscopy/spectroscopy

1. Introduction

Femtosecond Fourier-domain pulse shaping [1,2] continues to play a key role as an experimental tool in ultrafast sciences and has facilitated numerous exciting advances in many research fields. Some examples are quantum coherent control [3,4], femtosecond microscopy and spectroscopy [5,6], nonlinear fiber optics [7], high harmonic generation [8] and others.

In many cases, high-speed dynamic pulse-shape control is of primary importance. For example, in many adaptive techniques, browsing through the searchable space of parameters of the waveforms requires numerous iterations, and the pulse-shape update speed is often the rate-limiting element. In another example, fast switching between pulse shapes enables a lock-in microscopy technique [9], where the fast speed is critical to minimize noise and achieve high-resolution real-time imaging. These and other applications prompted the development of a variety of approaches for dynamic Fourier domain femtosecond pulse shaping. These included usage of one-dimensional (1D) liquid crystal SLMs [2], acousto-optic modulators [10], deformable mirrors [11], scanning over fixed masks [9] and electro-optical phased array modulators [12].

On the other hand, it is often desirable to be able to control not only spectral phases, but also spectral amplitudes of the femtosecond pulse. This capability is

particularly important for arbitrary waveform generation [13]. In principle, to achieve arbitrary temporal profiles, one has to control independently both spectral amplitudes and phases, as follows from the basic properties of the Fourier transform. In addition, independent phase and amplitude spectral control can be useful in nonlinear spectroscopy and microscopy, for instance, in the spectral hole refilling technique [14] for use in tissue microscopy. In this application, spectral amplitudes should be either completely blocked or a local oscillator (a few percent of the peak intensity) should be injected into the tailored spectral holes in a controlled way.

In the most ubiquitous approach, a one-dimensional array of liquid crystal (LC) elements is placed in the Fourier plane of the shaper [2]. This approach is often limited to a few tens of Hertz by the slow relaxation rate of the nematic LC. In acousto-optic modulators the acoustics grating wave is constantly moving in the modulator's aperture. Although, for every single femtosecond pulse, the acoustic wave appears frozen on the time scale of the pulse itself, the mask pattern changes on the timescale between successive pulses of a typical mode-locked oscillator. In fact, this restricts the usage of acousto-optic modulators to lower repetition rate sources such as femtosecond amplifiers. A deformable mirror shaper [11] is only able to provide smoothly varying phase

*Corresponding author. Email: eugene.frumker@nrc.ca

modulation due to the upper limit on curvature that can be induced in the membrane mirror. The scanning femtosecond pulse shaping [9] allows pulse shapes to be modulated at kilohertz rates but limits them to a predetermined set of static waveforms. Electro-optical gallium arsenide optical phased array modulators [12] provide a very high resolution and unsurpassed update rate on the nanosecond scale, but gallium arsenide has significant absorption at 800 nm, which makes it incompatible with Ti:Sapphire laser sources.

Amplitude modulation can be achieved with a single LC array with a polarizer by introducing light with appropriate input polarization relative to the liquid crystal axis. However, this also leads to coupled phase-modulation, which depends on the amplitude modulation level. Hence, for independent phase and amplitude control, two LC SLM arrays are used [15,13]. Although an advanced and efficient approach [13] is most popular today, it still has several inherent issues to be addressed. An extra modulator is required with its circuitry, bulkiness and very accurate mutual alignment between them. This usually doubles the system costs. Since the two modulators are physically separated (typically by several millimeters), the minimum single wavelength spot size is limited in order to ensure the Rayleigh range to be larger than this distance. Furthermore, the need for two polarizers results in additional losses and dispersion, and gratings used in the shaper exhibit significant polarization-dependent loss.

At the first glance, the femtosecond pulse shaping doesn't need more than one dimension. In fact, that was a way that most, if not all [16], femtosecond pulse shapers were designed [1] – the ultrashort pulse was angularly diffracted and each spectral color focused at a different position in the Fourier plane along a single dimension. In this paper, we will argue that the second dimension in the LC SLM can be used to effectively address both issues – to improve significantly the modulation speed [17] and the updatability of the generated waveforms; and on the other hand, to enable complex – spectral phases and amplitude modulation of the ultrafast waveforms [18].

2. High-rate scanning pulse shaping

Our 2D liquid crystal on silicon (LCOS) shaper set-up arrangement is shown in Figure 1.

The incident beam is reflected from the scanning mirror (SM) and is imaged by the telescope composed of lenses L1 and L2 ($f=100$ mm) onto a diffraction grating G (1200 mm^{-1}). The closed-loop scanner (CTI Model 6220) provides feedback reading of the

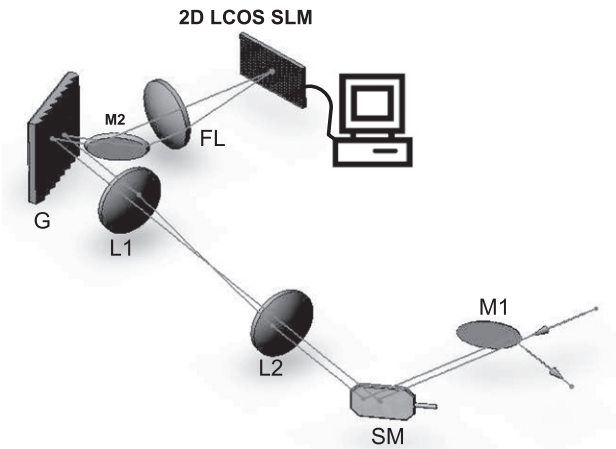


Figure 1. Schematic representation of the 2D LCOS SLM pulse shaper.

instantaneous angular position of the scanning mirror. This reading can be used for independent control of scanning amplitude and frequency as well as provide the reference signal for the pulse shape lock-in detection [9]. The diffracted beam, reflected close to the Littrow angle, is directed by mirror $M2$ into the Fourier pulse-shaper system composed of the spherical Fourier lens FL ($f=100$ mm) and LCOS SLM (Holoeye Model HEO1080P) in the Fourier plane. The LCOS SLM has 1920×1080 pixels with pixel pitch of $8\ \mu\text{m}$ and a fill-factor of almost 90%. The phase modulation SLM was checked and calibrated using a Michelson interferometer. The 2D SLM area was divided into two equal parts. The upper part was addressed with a particular gray scale value while the lower part was left intact. The interference fringes shift was recorded and the corresponding phase value retrieved. In this interferometric set-up it was also observed that the SLM is not perfectly flat, but rather has a slightly concave surface with about six to seven concentric fringes at 633 nm across the horizontal direction of the active area of the SLM, which corresponds to the radius of curvature of about 25 m. This causes a slight quadratic phase to be induced on the shaped pulse, but can be easily compensated for by shifting the SLM from the exact 4-f configuration. It was experimentally verified that with the horizontal polarization incident on the device, no noticeable parasitic amplitude modulation was observed. Given the shapers parameters we expect about $0.06\ \text{nm}/\text{pixel}$ resolution in near Littrow operation mode. This estimation was experimentally confirmed by repeatedly encoding a phase step along the SLM in different pixel positions and looking into spectral dips that are due to diffraction at the phase step. In this way we also accurately established pixel to wavelength

correspondence, which was used for spectral phase calculations and encoding across the SLM in the shaper. It was found to provide more than 2.5π phase modulation at 827 nm. The parasitic amplitude modulation did not exceed 4% over the entire phase modulation range, hence we can consider the device as a phase-only filter. The SLM was tilted slightly about the vertical axes, so that the zero diffraction order reflection was intercepted after the scanner with mirror M1. This tilt does not distort the pulse shape since it is equivalent to a linear spectral phase or a simple shift in the time domain. Actually a fast-scanning delay line was previously built with a similar system, but in the Fourier plane a simple scanning mirror [20,21] was placed instead of SLM.

There are three main routes to achieve dynamic pulse shape control with our shaper. In the first scheme, the scanning mirror is kept fixed and the updatability is achieved by refreshing the images on the SLM, as in a conventional LC based shaper. This classical scheme provides very high pulse synthesis fidelity with 1920 addressable pixels for spectral components modulation, but is limited by the slow update rate of the nematic LC – 60 Hz as stated by the manufacturer in our case; we experimentally found a 3 ms rise time.

In the second scheme, we divide the SLM into horizontal stripes. Each stripe encodes spectral phase information for a desired pulse shape. The stripe width is, of course, limited by the pixel size, but practically it was kept wider than the spot size in the Fourier plane. By rotating the scanner mirror, we sweep the horizontally diffracted spectral components in the vertical direction across the programmed stripes, thereby producing a multitude of different pulse shapes. In this scheme, the pulse shape update rate f_{pulse} is given by $f_{pulse} = 2 * f_{scan} * (A/d_{stripe} - 1)$, where f_{scan} is the scanning mirror frequency, A is the scanning peak-to-peak amplitude and d_{stripe} is the stripe width. As the f_{scan} is typically an order of magnitude larger than the typical refresh rate of the SLM, the highest pulse update rate f_{pulse} is achieved by keeping the stripe pattern fixed while scanning the mask. A straightforward combination of these two techniques can be particularly useful for a variety of nonlinear microscopy or spectroscopy applications. A slow SLM update can be used to change the pattern, while the very fast scanning pulse shape update can enable lock-in detection by switching between shapes [9].

Finally, it is possible to synchronize the scanning mirror position with the SLM refresh, so that each scan gets a new set of phase patterns. Although this approach would be slower by a factor $[f_{slm}/2f_{scan}]$ (where f_{slm} is the LC SLM refresh rate) as compared

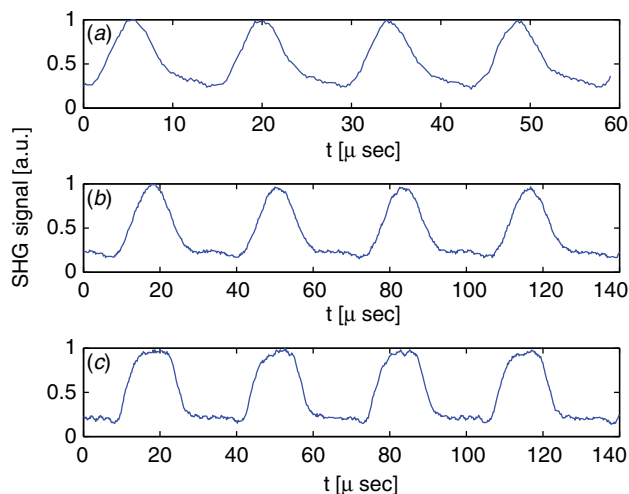


Figure 2. Update speed measurements. (a) Scanning rate 2200 Hz, 6 pixels stripe width. (b) Scanning rate 960 Hz, 6 pixels stripe width. (c) Scanning rate 1920 Hz, 12 pixels stripe width. (The color version of this figure is included in the online version of the journal.)

to the previous one, it facilitates generating completely arbitrary waveforms at a rate faster than f_{slm} alone by a factor of twice the number of dynamically encoded stripes. That could provide at least two orders of magnitude speed increase over the LC SLM alone. This scheme would be particularly suitable for adaptive techniques, which require numerous iterations for finding an optimal solution.

3. Phase and amplitude pulse shaping

Recently, the diffraction-based (first-order) method for shaping both spectral phases and amplitude by use of 2D SLM was introduced [16]. Here, we consider a zero-order approach for complex-spectral phases and amplitude modulation [18]. In this case, a cylindrical lens is used as the Fourier lens (FL) instead of a spherical lens and the scanner is kept static. Otherwise the shaper layout is the same as shown in Figure 2. The use of the cylindrical lens ensures that each wavelength component, while focused in the horizontal direction at the Fourier plane, extends over a few millimeters in the vertical direction. While the spectral components of the pulse are spread across the horizontal plane, we use the vertical direction for modulation of both spectral phases and amplitudes. By writing a vertical phase grating in each column of the SLM's two-dimensional matrix, we will achieve not only phase but also independent amplitude modulation control for the corresponding spectral component.

In the zero-order approach we encode the following phase function in the vertical direction (z) for each spectral component ω .

$$T(z, \omega) = \left[\text{rect}\left(\frac{z}{2z_0}\right) \cdot e^{i\left(A(\omega)\text{rect}\left(\frac{z}{z_0}\right) + B(\omega)\right)} \right] * \sum_{n=-\infty}^{+\infty} \delta(z - 2z_0n). \quad (1)$$

The complex transmittance $T(z, \omega) = e^{i\Phi(z, \omega)}$ is a periodic function in the z -dimension with period $P = 2z_0$.

Using Fourier decomposition in the vertical (z) direction, one can write:

$$T(z, \omega) = \sum_{n=-\infty}^{+\infty} C_n e^{i\frac{2\pi n}{P}z}. \quad (2)$$

The zero diffraction order of this phase grating corresponds to the zero-order in the Fourier expansion and is simply the average of the transmittance (1):

$$C_0(\omega) = \frac{1}{2z_0} \int_{-z_0}^{z_0} T(z, \omega) dz = \frac{1}{2} (1 + e^{iA(\omega)}) e^{iB(\omega)}. \quad (3)$$

The intensity of this zero diffraction order is given by

$$I_0 \sim |C_0(\omega)|^2 = \cos^2\left(\frac{A(\omega)}{2}\right). \quad (4)$$

We see that the amplitude modulation is solely determined by the phase contrast term $-A(\omega)$. Note that a full dynamic range of amplitude modulation of every frequency component is, in principle, possible by varying the $A(\omega)$ from 0 (no amplitude attenuation) to π (complete blockage) regardless the value of the phase DC term $-B(\omega)$. For a desired amplitude modulation $-\tau(\omega)$ and phase modulation $-\varphi(\omega)$ for a specific frequency component ω , the $A(\omega)$ and $B(\omega)$ can be determined from:

$$A(\omega) = 2 \arccos(\tau(\omega)) \quad (5)$$

$$B(\omega) = \varphi(\omega) - \arg(1 + e^{iA(\omega)}) = \varphi(\omega) - \frac{A(\omega)}{2}. \quad (6)$$

4. Experimental results

In all the experiments described below we used a home-built oscillator centered at 800 nm with a 30 nm spectral bandwidth. In the first experiment we checked the pulse shaping capability of the system. First, we simply encoded a phase pattern to compensate for the residual dispersion experienced by the beam as it passes through the many dispersive elements in our set-up. This is done by maximizing a second harmonic signal from a 20 micron BBO crystal, while searching for the

spectral phase polynomial containing GVD and third-order dispersion terms with a direct search algorithm.

To check the update rate of the shaper we encoded two types of alternating horizontal stripes. One stripe contained the spectral phase needed for dispersion correction, which led to a transform limited pulse. The other stripe was encoded with a sinusoidal spectral phase with a period of about 1.55 THz. We verified that this periodic modulation reduces the second harmonic generated signal by more than factor of four as compared with the transform limited pulse, while the light intensity was reduced by less than 2%. The entire 2D aperture of the SLM was filled with the alternating stripes mask. We then scanned the mirror with triangle modulation signal to guarantee equal time spacing. The positioning and the current feedback available from the scanner was monitored by a digital oscilloscope along with the PMT output measuring the SHG signal. The PMT output was amplified with low-noise pre-amp model SRS560 and acquired by the oscilloscope in the averaging mode (100 times) to reduce the noise.

In Figure 2(a) the resulting SHG signal is shown as the function of time. In this case the scanning mirror frequency was set to 2200 Hz and the stripe width was 6 pixels wide (about 50 μm). The pulse shape update rate achieved in this case is about 140 kHz, which is at least three orders of magnitude faster than the best LC SLMs. In this particular case, the stripe width was close to the spot size in the Fourier plane (about 30 μm). Intersection of this spot with the edges of the stripe causes diffraction and reduction of the SHG signal. That explains the relatively sharp peaks in Figure 2(a). Note the difference between the 6 pixel-width with 960 Hz scanning frequency and 12 pixel-width with 1920 Hz shown in Figures 2(b) and (c), respectively. While both cases result in the same modulation frequency of about 62 kHz, the 6 pixel-width case has consistently sharper peaks. The slight undershooting at the start of each pulse is attributed to the diffraction loss from the stripes adjacent edges, superimposed with a small impedance mismatch in the detection electronics.

To test the phase and amplitude shaping capability in the zero-order operation, we encoded different periodic phase and amplitude functions following the procedure described in Section 3. We measured that LCOS 2D SLM efficiency in the zero-order is $\sim 67\%$, as compared with $\sim 43\%$ found in the first-order operations scheme.

The output from the shaper was directed via a chopper into the signal arm of non-collinear cross-correlator. The reference unshaped beam sampled by a 50% beam-splitter and signal beam were focused by a spherical mirror ($f = 100$ mm) into 20 μm BBO

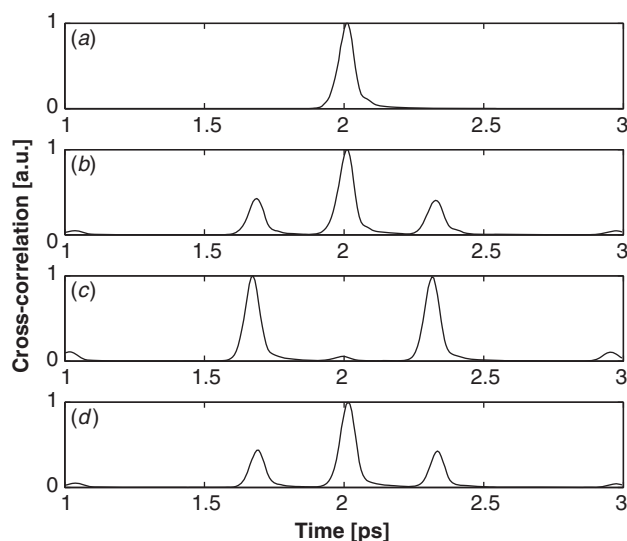


Figure 3. Experimental results for cross-correlation for zero-order approach. (a) No phase is applied. (b) Periodic phase only modulation with binary modulation depth of $\pi/2$ and period 3.1 THz. (c) Periodic phase only modulation with modulation depth of π . (d) Periodic amplitude only modulation.

crystal and the second harmonic signal was filtered and detected by photomultiplier tube (PMT Hamamatsu model 1P28) and fed into a lock-in amplifier (Signal Recovery 7265) referenced to the chopper modulation frequency. Typical results are shown in Figure 3. Figure 3(a) shows the cross-correlation result with no modulation applied on the SLM. The cross-correlation pulse width is practically Fourier limited with a slight asymmetric tail indicating some small residual third-order spectral phase. In Figure 3(b) the cross-correlation result is shown for binary-periodic-phase-only modulation. Such periodic phase modulation should produce a series of pulses with vanishing even temporal orders. This relative amplitude distribution is further apodized as a result of the finite spot size in the Fourier plane [1]. In Figure 3(b) the three central cross-correlation peaks are due to the zero and first orders. The small peaks seen at the beginning and the end of the picture are due to the third temporal order as the second order vanishes. The period of this modulation was 3.1 THz and the distance between zero-order and first-order temporal satellites was measured as ~ 320 fs as expected. In Figure 3(c) the cross-correlation trace is shown for the same phase-only periodic spectral mask, but with modulation depth of π . For this modulation depth one would expect complete cancellation of zero-order replica ($I_0 \sim \cos^2(\varphi/2)$, where I_0 is the intensity of temporal zero-order and φ is the phase modulation depth) in the time domain. In Figure 3(c) we can clearly see that the residual zero-order pulse replica persists in the time

domain. The height of this zero-order peak in the cross correlation trace is about 0.05 of the first-order peak. It means that at most 2.5% of the total intensity goes to the first-order (even neglecting higher than first-order temporal satellites). We attribute this zero-order intensity to the problem of the ‘flicker’ – a parasitic time-dependent modulation of the device at about 300 Hz, that we found experimentally in our SLM. It turned out that this problem is the result of the electronic modulation scheme applied by the manufacturer in the device, and is not a real physical limitation of the LCOS display technology. This indicates that ‘dead zones’ do not contribute to the temporal zero-order in the cross-correlation trace. In Figure 3(d) the cross-correlation result is shown for binary-periodic-amplitude-only modulation. This periodic amplitude modulation should result in a series of pulses similar to the phase-only modulation case, but with relative intensities proportional now to $\text{sinc}^2(n/2)$ for the n th temporal order pulse, further apodized as the result of the finite spot size. In Figure 3(d) we see that even orders vanish, as follows from analytical prediction, and the experimentally measured first and third orders have intensity 0.42 and 0.045 relative to the zero-order intensity – in very good argument with the theoretically expected result. Note that in the case of amplitude modulation, the zero order amplitude is always larger than that of higher orders, while in the periodic phase modulation case the energy distribution between zero and higher orders can be continuously controlled up to complete vanishing of the zero-order pulse as in Figure 3(c). It is also clear that in the amplitude modulation case the total intensity is attenuated, while for phase only modulation the intensity is preserved.

5. Conclusions

We have considered two-dimensional SLM for dynamic, phase and amplitude pulse shaping. It has been shown, both theoretically and experimentally, that the second dimension can be used to drastically increase the femtosecond pulse shaping update rate as well as to provide complex (phase and amplitude) pulse shaping capability with phase only SLM.

We experimentally demonstrated a speed increase of almost four orders of magnitude over a typical LC SLM shaper, while providing very high fidelity in pulse shape synthesis. We believe that the unique combination of extremely fast speed, very high fidelity and robustness could have a significant impact in diverse fields of femtosecond research. A combination of this technique with faster scanning polygon mirrors may lead to megahertz update rate shaping. Usage

of micromirror SLM [24] instead of LC SLM in the combined scheme for arbitrary waveform generation will lead to at least another order of magnitude update rate increase.

A zero-order approach was presented, theoretically analyzed and experimentally proved to have a significantly higher light efficiency than the first-order approach, and to be inherently free of vertical angular frequency chirp. In the future studies, given the superior pixel count and constantly improving quality of modern 2D SLM modulators, the presented techniques can be combined to achieve both an arbitrary waveform generation and significantly enhanced update rate. We believe that the presented modulation techniques with 2D SLM in addition with other methodologies [22,23] of using the 2D SLM in pulse shaping, will prompt the active usage of two-dimensional modulators in a variety of ultrafast science frontiers.

References

- [1] Weiner, A.M. *Rev. Sci. Instrum.* **2000**, *71*, 1929–1960.
- [2] Weiner, A.M.; Leaird, D.E.; Patel, J.S.; Wullert II, J.R. *Opt. Lett.* **1990**, *15*, 326–328.
- [3] Assion, A.; Baumert, T.; Bergt, M.; Brixner, T.; Kiefer, B.; Seyfried, V.; Strehle, M.; Gerber, G. *Science* **1998**, *282*, 919–922.
- [4] Meshulach, D.; Silberberg, Y. *Nature* **1998**, *396*, 239–242.
- [5] Tian, P.; Keusters, D.; Suzaki, Y.; Warren, W.S. *Science* **2003**, *300*, 1553–1555.
- [6] Dudovich, N.; Oron, D.; Silberberg, Y. *Nature* **2002**, *418*, 512–514.
- [7] Efimov, A.; Taylor, A.J.; Omenetto, F.G.; Vanin, E. *Opt. Lett.* **2004**, *29*, 271–273.
- [8] Bartels, R.; Backus, S.; Zeek, E.; Misoguti, L.; Vdovin, G.; Christov, I.P.; Murnane, M.M.; Kapteyn, H.C. *Nature* **2000**, *406*, 164–166.
- [9] Frumker, E.; Oron, D.; Mandelik, D.; Silberberg, Y. *Opt. Lett.* **2004**, *29*, 890–892.
- [10] Hillegas, C.W.; Tull, J.X.; Goswami, D.; Strickland, D.; Warren, W.S. *Opt. Lett.* **1994**, *19*, 737–739.
- [11] Zeek, E.; Maginnis, K.; Backus, S.; Russek, U.; Murnane, M.; Mourou, G.; Kapteyn, H.; Vdovin, G. *Opt. Lett.* **1999**, *24*, 493–495.
- [12] Frumker, E.; Tal, E.; Silberberg, Y.; Majer, D. *Opt. Lett.* **2005**, *30*, 2796–2798.
- [13] Wefers, M.M.; Nelson, K.A. *Opt. Lett.* **1995**, *20*, 1047–1049.
- [14] Fischer, M.C.; Ye, T.; Yurtsever, G.; Miller, A.; Ciocca, M.; Wagner, W.; Warren, W.S. *Opt. Lett.* **2005**, *30*, 1551–1553.
- [15] Wefers, M.M.; Nelson, K.A. *Opt. Lett.* **1993**, *18*, 2032–2034.
- [16] Vaughan, J.C.; Hornung, T.; Feurer, T.; Nelson, K.A. *Opt. Lett.* **2005**, *30*, 323–325.
- [17] Frumker, E.; Silberberg, Y. *Opt. Lett.* **2007**, *32*, 1384–1386.
- [18] Frumker, E.; Silberberg, Y. *J. Opt. Soc. Am. B* **2007**, *24*, 2940–2947.
- [19] Goodman, J.W. *Introduction to Fourier Optics*; McGraw-Hill: Boston, MA, 1996.
- [20] Kwong, K.; Yankelevich, D.; Chu, K.; Heritage, J.; Dienes, A. *Opt. Lett.* **1993**, *18*, 558–560.
- [21] Tearney, G.J.; Bouma, B.E.; Fujimoto, J.G. *Opt. Lett.* **1997**, *22*, 1811–1813.
- [22] Feurer, T.; Vaughan, J.C.; Koehl, R.M.; Nelson, K.A. *Opt. Lett.* **2002**, *27*, 652–654.
- [23] Feurer, T.; Vaughan, J.C.; Nelson, K.A. *Science* **2003**, *299*, 374–377.
- [24] Hacker, M.; Stobrawa, G.; Sauerbrey, R.; Buckup, T.; Motzkus, M.; Wildenhain, M.; Gehner, A. *Appl. Phys. B* **2003**, *76*, 711–714.